JOURNAL OF COMPUTATIONAL PHYSICS 54, 205–220 (1984)

An Implicit Scheme for Calculating Time- and Frequency-Dependent Flux Limited Radiation Diffusion in One Dimension*

TIMOTHY S. AXELROD, PAUL F. DUBOIS, AND CLIFFORD E. RHOADES, JR.

Lawrence Livermore National Laboratory, Livermore, California 94550

Received April 5, 1983; revised June 23, 1983

A flexible and accurate method for solving nonlinear time- and frequency-dependent flux-limited radiation diffusion and radiation-matter coupling problems in one dimension is developed. The method is based on converting the set of partial differential equations for the flux-limited multigroup diffusion approximation into a system of ordinary differential equations which are integrated by a generalized stiff equation solver. Unlike previous operator-splitting techniques which can introduce instabilities into the solution or which produce smooth but highly inaccurate solutions, this scheme provides a reliable accurate solution with reduced overall computational effort. The solutions describe both the streaming and diffusion limits of transport theory and are stable with time steps comparable to the changes in physical variables.

INTRODUCTION

The multigroup flux-limited diffusion approximation to the radiative transfer equation is an efficient and relatively inexpensive approach which has been widely used in various applications. Pioneering research of LeBlanc and Wilson in the early 1970s was first used by Alme and Wilson [1] to study x-ray emission from neutron stars. As is well known, approximate treatment of the transfer equation may result in serious errors for some problems. Less widely appreciated is the fact that significant further errors can be introduced by the algorithm used to implement the method. These errors typically arise from applying operator splitting techniques without restricting the time step sufficiently to ensure accurate treatment of a wide variety of nonlinear processes that may be present. To overcome some of these difficulties, Lund and Wilson [2] have devised an iterative matrix-inversion technique for solving one-dimensional time-dependent multifrequency radiation transport problems. In this paper, we present an implementation of the multigroup diffusion approximation in one dimension which uses a general stiff ordinary differential equation solver to control errors systematically while permitting relatively large time steps to be taken.

* Work performed under the auspices of the U. S. Department of Energy by the Lawrence Livermore National Laboratory Contract W-7405-ENG-48.

0021-9991/84 $3.00

This method has been found to be superior to operator splitting with respect to accuracy, reliability, and efficiency.

The outline of the paper is as follows. In Section I, the physical model of the radiative transfer equation is presented. Section II is devoted to details of the solution of the problem, which turns out to be quite straightforward. Some numerical illustrations are provided in Section III. Finally, Section IV contains a summary of our experience with the model.

I. Physical Model

The general radiation transport problem is to describe the radiation field as a function of direction, frequency, and position in space. In general, the radiation field has units of energy/volume-steradian-frequency. For simplicity, we take a one-dimensional Lagrange viewpoint with discretized frequency groups. In the following text, units for the dependent and independent variables are indicated in curly braces. Naturally, any consistent set of units may be used.

A model using a one-dimensional Lagrangian mesh with spherical, cylindrical, or planar symmetry and discretized frequency groups has independent variables,

x_j: spatial coordinate of the jth interface $(j = 1, J)$ {cm},
v_g: center energy of the gth photon group $(g = 1, G)$ {keV},
t: time {sec}.

The range of the various indices are indicated above in parentheses. The dependent variables, all of which are zone centered, are

$u_{gj+1/2}$: photon energy density contained in the gth group for the jth zone {erg cm^{-3}},
$\theta^{\mathrm{i}}_{j+1/2}$: ion temperature in the jth zone {keV},
$\theta^{\mathrm{e}}_{j+1/2}$: electron temperature in the jth zone {keV}.

Within each zone, all quantities are assumed to be independent of position. Similarly, all quantities are assumed to be independent of photon energy within a group.

The dynamical equations, before spatial discretization, are

$$\frac{\partial u_g}{\partial t} = -\nabla \cdot F^r_g + c\sigma^{\mathrm{a}}_g(\theta^{\mathrm{e}})[B_g(\theta^{\mathrm{e}}) - u_g] + S_g + W_g \qquad (g = 1, G), \tag{1.1}$$

$$\rho c^{\mathrm{e}}_{\mathrm{v}} \frac{\partial \theta^{\mathrm{e}}}{\partial t} = -\nabla \cdot F^{\mathrm{e}} - c \sum_{g=1}^{G} \sigma^{\mathrm{a}}_g(\theta^{\mathrm{e}})[B_g(\theta^{\mathrm{e}}) - u_g] - \sum_{g=1}^{G} S_g + \omega^{\mathrm{ie}}(\theta^{\mathrm{e}}) \cdot (\theta^{\mathrm{i}} - \theta^{\mathrm{e}})\, c^{\mathrm{i}}_{\mathrm{v}}\rho + S^{\mathrm{e}}/\rho, \tag{1.2}$$

$$\rho c^{\mathrm{i}}_{\mathrm{v}} \frac{\partial \theta^{\mathrm{i}}}{\partial t} = -\nabla \cdot F^{\mathrm{i}} + \omega^{\mathrm{ie}}(\theta^{\mathrm{e}}) \cdot (\theta^{\mathrm{e}} - \theta^{\mathrm{i}}) \cdot c^{\mathrm{i}}_{\mathrm{v}}\rho + S^{\mathrm{i}}/\rho. \tag{1.3}$$

The following quantities have been introduced:

c: speed of light $\{\text{cm sec}^{-1}\}$,

$B_g(\theta)$: integral of the Planck function at temperature θ over group g $\{\text{erg cm}^{-3}\}$,

F_g^r: photon energy flux for group g $\{\text{erg cm}^{-2}\ \text{sec}^{-1}\}$,

F^e, F^i: energy flux from electron and ion heat conduction $\{\text{erg cm}^{-2}\ \text{sec}^{-1}\}$,

S_g: energy rate into group g from Compton scattering with thermal electrons $\{\text{erg cm}^{-3}\ \text{sec}^{-1}\}$,

W_g: energy rate into group g from hydrodynamic work on radiation $\{\text{erg cm}^{-3}\ \text{sec}^{-1}\}$,

c_v^e, c_v^i: specific heat at constant volume for electrons and ions $\{\text{erg } g^{-1}\ \text{keV}^{-1}\}$,

ρ: matter density $\{g\ \text{cm}^{-3}\}$,

σ_g^a: macroscopic absorption cross section for photons of frequency ν_g, corrected for stimulated emission $\{\text{cm}^{-1}\}$,

S^e, S^i: energy rate from hydrodynamic work and external sources to electrons and ions $\{\text{erg } g^{-1}\ \text{sec}^{-1}\}$,

ω^{ie}: ion–electron coupling rate $\{\text{sec}^{-1}\}$.

Derivations of the appropriate Lagrangian transport equations have been given by Castor [3], using Lindquist's formalism [4], and by Buchler [5], using invariance of the photon-Boltzmann equation. Both Castor and Buchler work in a Lagrangian frame and only carry terms in one order of v/c. Equation (1.1) is a further simplification which is entirely adequate in the diffusion approximation. Steps leading to Eq. (1.1) involve the cancellation of certain v/c terms and neglect of others. Where the material velocity (v) is small compared with the speed of light, one can properly neglect v/c terms in the equation of transfer. Further, where the opacity is continuous and spectral lines are ignorable, it is often sufficient to obtain solutions to the transfer equation by omitting v/c terms.

We have chosen to use the Lagrangian frame of reference because it is the natural frame for specifying fluid thermodynamic properties. Moreover, it is the frame in which atomic absorption and emission are isotropic and in which the equation for Compton scattering can be written easily. Although the diffusion limit corresponds to a very low order approximation in both frequency and angle, as well as space and time, it is widely used in many radiation-hydrodynamic calculations because of its inherent simplicity. Surprisingly, in view of all the approximations made, it is a reasonably accurate description in many situations, correctly giving gross features of the radiation flow in both a qualitative and a quantitative sense.

Any diffusion equation such as Eq. (1.1) has an infinite speed of propagation and consequently tends to predict too large a radiative flux. For these reasons, a flux-limiting approach is used in the present work. The radiative fluxes F_g^r are calculated by flux-limited diffusion,

$$F_g^r = D_g^r \nabla u_g, \tag{1.4}$$

where the diffusion coefficients D_g^r incorporate a flux limiter due to Wilson,

$$D_g^r = c \Big/ \left[3\sigma_g^a \min\left(\frac{B_g}{u_g}, 1\right) + 3\sigma_g^s + \frac{1}{u_g}\left|\frac{\partial u_g}{\partial x}\right| \left(1 + 3\exp\left\{ -\frac{0.5}{\sigma_g^t}\left(\frac{1}{u_g}\left|\frac{\partial u_g}{\partial x}\right| + \frac{3.6}{x}\right)\right\}\right)\right], \quad (1.5)$$

which interpolates between the diffusion and free streaming limits in an ad hoc fashion. The $1/x$ term is present only for spherical geometry. Here, σ^a, σ^s, and σ^t are the absorption, scattering, and total photon cross sections. More recently, Levermore [6] has derived a more physically rigorous form for the flux limiter. Many other flux limiters have been suggested and it is difficult, if not impossible, to single out one as preferred. Which performs best may well be problem dependent. A comparison of various flux limiters including those of Wilson has been made by Pomraning [7, 8]. A broader view of flux-limited diffusion theory has been provided by Levermore and Pomraning [9] and consequently will not be discussed here.

The difference formula for evaluating the radiative fluxes at zone interfaces incorporates a combination of optical depth averaging (for the diffusion limit) and upstream differencing (for the free streaming limit). After differencing, the radiative fluxes are

$$F_{gj}^r = a_{gj}^r (u_{gj-1/2} - u_{gj+1/2}). \quad (1.6)$$

The electron and ion heat fluxes are also approximated by flux-limited diffusion and similarly differenced to yield

$$F_j^e = a_j^e(\theta_{j-1/2}^e - \theta_{j+1/2}^e), \qquad F_j^i = a_j^i(\theta_{j-1/2}^i - \theta_{j+1/2}^i). \quad (1.7)$$

We note that the flux coefficients a_{gj}^r depend on $u_{gj-1/2}$ and $u_{gj+1/2}$, although this dependence is not explicitly indicated. Similar dependencies are present for a_j^e and a_j^i. Vacuum boundaries are simply modeled by including a "phantom" zone at each end of the Lagrangian mesh. These zones have specified photon energy densities, infinite radiative mean free paths, and zero heat conductivities.

The flux divergences which occur in Eqs. (1.1)–(1.3) are zone centered and evaluated in terms of the interface fluxes as

$$-(\nabla \cdot F)_{j+1/2} = \frac{1}{V_{j+1/2}} [A_j F_j - A_{j+1} F_{j+1}], \quad (1.8)$$

where we have defined

$V_{j+1/2}$: volume of the jth zone $\{\text{cm}^3\}$,

A_j: area of the jth interface $\{\text{cm}^2\}$.

The hydrodynamic work on radiation is approximated by

$$W_g = -(\gamma - 1)\frac{1}{V}\frac{\partial V}{\partial t}u_g, \tag{1.9}$$

where γ is the radiation gamma which in the pure diffusion limit is just the well-known $\gamma = \frac{4}{3}$ adiabatic compression. Our techniques for differencing the radiative, electron, and ion heat fluxes, and for averaging the diffusion coefficients are standard. Lund and Wilson [2] have discussed them in detail and consequently we do not address them here.

The calculation of the Compton energy rate S_g requires some discussion. Previous implementations of multigroup diffusion which included Compton scattering [10, 11] have utilized the Kompaneets equation [12], for which the independent variable is the photon mode occupation number n_g. The method we have developed requires that the Compton term S_g be treated simultaneously with the rest of Eq. (1.1), so that it must be expressed in terms of the u_g. Although there is a simple relation between n_g and u_g,

$$n_g = \beta_g u_g = \frac{(hc)^3}{8\pi}\frac{1}{v_g^3 \Delta v_g}u_g, \tag{1.10}$$

it is more convenient to express S_g directly in a transfer matrix form than to transform the Kompaneets equation to the new variables. Stone [13] and Winslow [14] have discussed the relationship of the two approaches.

To develop the appropriate form for S_g we note that as differenced by Chang and Cooper [15] the Kompaneets equation couples only nearest neighbor groups. Retaining this coupling and requiring that the Compton operator conserve photon number which we define as

$$G_{\text{phot}} = \sum_{g=1}^{G}\frac{u_g}{v_g}, \tag{1.11}$$

results in

$$S_g = c\left[\sigma_{g-1}^{+}\frac{v_g}{v_{g-1}}u_{g-1}(\beta_g u_g + 1) - \sigma_g^{-}u_g(\beta_{g-1}u_{g-1} + 1)\right.$$
$$\left. - \sigma_g^{+}u_g(\beta_{g+1}u_{g+1} + 1) + \sigma_{g+1}^{-}\frac{v_g}{v_{g+1}}u_{g+1}(\beta_g u_g + 1)\right]. \tag{1.12}$$

The cross sections for up and down scatter σ_g^{+} and σ_g^{-} are completely determined by the requirements that the energy transfer rate agree with that determined from numerical integration of the Compton energy transfer cross section, and that the proper Bose–Einstein distribution be the steady state solution. The $(\beta u + 1)$ terms account for stimulated scattering and make the scattering term nonlinear in u, although this is rarely important.

The dynamical equations (1.1)–(1.3), after spatial differencing and inclusion of the explicit forms for S_g and W_g, become

$$\begin{aligned}
\dot{u}_{gj+1/2} = {} & \frac{1}{V_{j+1/2}} [A_j a^r_{gj}(u_{gj-1/2} - u_{gj+1/2}) - A_{j+1} a^r_{gj+1}(u_{gj+1/2} - u_{gj+3/2})] \\
& + c\sigma^{\mathrm{a}}_{gj+1/2}(\theta^{\mathrm{e}}_{j+1/2})[B_g(\theta^{\mathrm{e}}_{j+1/2}) - u_{gj+1/2}] \\
& + c\Big[\sigma^{+}_{g-1,j+1/2}(\theta^{\mathrm{e}}_{j+1/2}) \frac{v_g}{v_{g-1}} u_{g-1,j+1/2}(\beta_g u_{gj+1/2} + 1) \\
& - \sigma^{-}_{gj+1/2}(\theta^{\mathrm{e}}_{j+1/2})\, u_{gj+1/2}(\beta_{g-1} u_{g-1,j+1/2} + 1) \\
& - \sigma^{+}_{gj+1/2}(\theta^{\mathrm{e}}_{j+1/2})\, u_{gj+1/2}(\beta_{g+1} u_{g+1,j+1/2} + 1) \\
& + \sigma^{-}_{g+1,j+1/2}(\theta^{\mathrm{e}}_{j+1/2}) \frac{v_g}{v_{g+1}} u_{g+1,j+1/2}(\beta_g u_{gj+1/2} + 1)\Big] \\
& - (\gamma_{gj+1/2} - 1) \frac{1}{V_{j+1/2}} \frac{dV_{j+1/2}}{dt} u_{gj+1/2}, \qquad (1.13)
\end{aligned}$$

$$\begin{aligned}
\dot{\theta}^{\mathrm{e}}_{j+1/2} = {} & \frac{1}{\rho_{j+1/2} c^{\mathrm{e}}_{vj+1/2}} \Big\{ \frac{1}{V_{j+1/2}} [A_j a^{\mathrm{e}}_j(\theta^{\mathrm{e}}_{j-1/2} - \theta^{\mathrm{e}}_{j+1/2}) \\
& - A_{j+1} a^{\mathrm{e}}_{j+1}(\theta^{\mathrm{e}}_{j-1/2} - \theta^{\mathrm{e}}_{j+3/2})] \\
& - \sum_{g=1}^{G} c\sigma^{\mathrm{a}}_{gj+1/2}(\theta^{\mathrm{e}}_{j+1/2})[B_g(\theta^{\mathrm{e}}_{j+1/2}) - u_{gj+1/2}] \\
& - \sum_{g=1}^{G} c\Big[\sigma^{+}_{g-1,j+1/2}(\theta^{\mathrm{e}}_{j+1/2}) \frac{v_g}{v_{g-1}} u_{g-1,j+1/2}(\beta_g u_{gj+1/2} + 1) \\
& - \sigma^{-}_{gj+1/2}(\theta^{\mathrm{e}}_{j+1/2})\, u_{gj+1/2}(\beta_{g-1} u_{g-1,j+1/2} + 1) \\
& - \sigma^{+}_{gj+1/2}(\theta^{\mathrm{e}}_{j+1/2})\, u_{gj+1/2}(\beta_{g+1} u_{g+1,j+1/2} + 1) \\
& + \sigma^{-}_{g+1,j+1/2}(\theta^{\mathrm{e}}_{j+1/2}) \frac{v_g}{v_{g+1}} u_{g+1,j+1/2}(\beta_g u_{gj+1/2} + 1)\Big]\Big\} \\
& + \omega^{\mathrm{ie}}_{j+1/2} \frac{c^n_{vj+1/2}}{c^{\mathrm{e}}_{vj+1/2}} (\theta^{\mathrm{i}}_{j+1/2} - \theta^{\mathrm{e}}_{j+1/2}) + \frac{S^{\mathrm{e}}_{j+1/2}}{c^{\mathrm{e}}_{vj+1/2}}, \qquad (1.14)
\end{aligned}$$

$$\begin{aligned}
\dot{\theta}^{\mathrm{i}}_{j+1/2} = {} & \frac{1}{\rho_{j+1/2} c^n_{vj+1/2}} \Big\{ \frac{1}{V_{j+1/2}} [A_j a^{\mathrm{i}}_j(\theta^{\mathrm{i}}_{j-1/2} - \theta^{\mathrm{i}}_{j+1/2}) \\
& - A_{j+1/2} a^{\mathrm{i}}_{j+1}(\theta^{\mathrm{i}}_{j+1/2} - \theta^{\mathrm{i}}_{j+3/2})]\Big\} \\
& + \omega^{\mathrm{ie}}_{j+1/2}(\theta^{\mathrm{e}}_{j+1/2} - \theta^{\mathrm{i}}_{j+1/2}) + \frac{S^{\mathrm{i}}_{j+1/2}}{c^n_{vj+1/2}}. \qquad (1.15)
\end{aligned}$$

The physical model is thus represented by a large set of ordinary differential equations, with typical problems having between 100 and 10,000. These equations have a wide variety of nonlinearities. Although some of these are explicitly present, for example, in the temperature dependence of $B_g(\theta)$, others result from coupling with other physical processes. Examples of the latter include strongly temperature-dependent source rates resulting from thermonuclear reactions and temperature dependence of absorption cross sections. There are many others. We note further that the equations are typically very stiff, with characteristic timescales spanning many orders of magnitude, and have a fairly complex cross-coupling pattern.

II. The Integration Method

Our model solution is evolved in time using a variant of Alan Hindmarsh's GEARBI [16] package. This package is one of the Gear [17] family of codes and is well documented. We had to vary the usual Gear predictions for θ^e to improve the likelihood of convergence in the nonlinear solver.

For those not familiar with the method, a rough sketch is in order. The current solution vector $y(t)$ is advanced by predicting a value $\hat{y}(t+\Delta t)$. This value is then "corrected" by solving a nonlinear equation. The prediction and correction depend on the "order" the method is using. The order varies from 1 to 5 and is the degree of the polynomial which defines the predicted and corrected values. At first order, for example, in solving $\dot{y} = f(y, t)$ we would have $\hat{y}(t+\Delta t) = y(t) + \Delta t f(y, t)$ and solve for $y(t+\Delta t)$ by solving the backward Euler equation,

$$y(t+\Delta t) - y(t) = \Delta t f[\, y(t+\Delta t), t+\Delta t].$$

At higher orders more than one past solution vector is used but the idea is the same. One important fact is that at any order, the Jacobian of the nonlinear problem consists of some diagonal matrix plus the Jacobian $\partial f/\partial y$, and thus has the same sparsity pattern.

The order and Δt are adjusted so that the approximate local error in going from t to $t+\Delta t$ is bounded in norm by a user-supplied tolerance. The order and Δt are chosen so that this tolerance is met and Δt is as large as possible. Whenever Δt changes, an interpolation is used to get data at the new spacing. There are some heuristic rules to prevent too frequent changes in order and Δt, especially the latter since the Gear method is at heart a fixed-step algorithm. We now feel that use of a truly variable step method like TORANAGA [18] might be superior since we usually have to pay most of the penalties associated with those methods anyway.

The nonlinear solver typically calls a linear solver and there ensues considerable discussion between the integrator, nonlinear solver, and linear solver until a Δt and order have been found which enables all of them to satisfy their respective error criteria. The most difficult part of using this method is the design of a suitable linear solver, and writing and debugging the subroutines for $f(y, t)$ and $\partial f/\partial y$.

A. *Solution of the Nonlinear Problem*

The nonlinear problem posed by the integrator is solved by Newton's method. The only variation is whether we evaluate the Jacobian matrix at each iterate or trial solution ("full" Newton) or use the Jacobian at some previous solution iterate or time step ("modified" Newton). Modified Newton is used until a failure occurs (i.e., the linear solver fails or convergence does not occur). If the Jacobian is out of date, it is updated and we try again. If the Jacobian is up-to-date, and failure occurs anyway, we judge that the problem has become "hard" and switch to the full Newton method. When failure occurs with the full-Newton integrator, we cut the time step (Δt) size.

As a further wrinkle, it is possible to try returning to modified Newton after a while to see if the problem has "relaxed."

To apply the ordinary differential equation solver to the physics model given by Eqs. (1.13)–(1.15), the dependent variables are arranged as a single vector with the ordering,

$$y = \{u_{1,1/2}u_{2,1/2},\ldots, u_{G,1/2}, \theta^{\mathrm{i}}_{1/2}, \theta^{\mathrm{e}}_{1/2}, u_{1,3/2}, u_{2,3/2},\ldots$$
$$\theta^{\mathrm{e}}_{3/2},\ldots, u_{1J+1/2},\ldots, u_{GJ+1/2}\theta^{\mathrm{i}}_{J+1/2}\theta^{\mathrm{e}}_{J+1/2}\}.$$

The number of groups is G, as previously, while J is the number of spatial zones plus two (to account for the phantom zones at the two boundaries). The Jacobian matrix C which is needed for the Newton iteration is formed in a straightforward way from Eqs. (1.13)–(1.15), although a number of approximations are made. The nonzero Jacobian elements are

$$\frac{\partial \dot{u}_{gj+1/2}}{\partial u_{gj-1/2}} = \frac{A_j}{V_{j+1/2}}\left[a^r_{gj} + (u_{gj-1/2} - u_{gj+1/2})\frac{\partial a^r_{gj}}{\partial u_{gj-1/2}}\right],$$

$$\frac{\partial \dot{u}_{gj+1/2}}{\partial u_{g-1,j+1/2}} = c\left[\sigma^{+}_{g-1,j+1/2}(\theta^{\mathrm{e}}_{j+1/2})\frac{v_g}{v_{g-1}}(\beta_g u_{gj+1/2} + 1)\right.$$
$$\left. - \beta_{g-1}\sigma^{-}_{gj+1/2}u_{gj+1/2}\right],$$

$$\frac{\partial \dot{u}_{gj+1/2}}{\partial u_{gj+1/2}} = -\frac{1}{V_{j+1/2}}\left\{A_j\left[a^r_{gj} - (u_{gj-1/2} - u_{gj+1/2})\frac{\partial a^r_{gj}}{\partial u_{gj+1/2}}\right]\right.$$
$$\left. + A_{j+1}\left[a^r_{gj+1} - (u_{gj+1/2} - u_{gj+3/2})\frac{\partial a^r_{gj+1}}{\partial u_{gj+1/2}}\right]\right\}$$
$$- c\sigma^{\mathrm{a}}_{gj+1/2}(\theta^{\mathrm{e}}_{j+1/2}) - c[\sigma^{-}_{gj+1/2}(\theta^{\mathrm{e}}_{j+1/2})(\beta_{g-1}u_{g-1,j+1/2} + 1)$$
$$+ \sigma^{+}_{gj+1/2}(\theta^{\mathrm{e}}_{j+1/2})(\beta_{g+1}u_{g+1,j+1/2} + 1)$$
$$- \beta_g\sigma_{g+1,j+1/2}(\theta^{\mathrm{e}}_{j+1/2})\frac{v_g}{v_{g+1}}u_{g+1,j+1/2}$$

$$- \beta_g \sigma^+_{g-1,j+1/2}(\theta^e_{j+1/2}) \frac{v_g}{v_{g-1}} u_{g-1,j+1/2}$$

$$- (\gamma_{gj+1/2} - 1) \frac{1}{V_{j+1/2}} \frac{dV_{j+1/2}}{dt},$$

$$\frac{\partial \dot{u}_{gj+1/2}}{\partial u_{g+1,j+1/2}} = c \left[\sigma^-_{g+1,j+1/2}(\theta^e_{j+1/2}) \frac{v_g}{v_{g+1}} (\beta_g u_{gj+1/2} + 1) \right.$$

$$\left. - \beta_{g+1} \sigma^+_{gj+1/2}(\theta^e_{j+1/2}) u_{gj+1/2} \right],$$

$$\frac{\partial \dot{u}_{gj-1/2}}{\partial \theta^e_{j+1/2}} = c\sigma^a_{gj+1/2}(\theta^e_{j+1/2}) \frac{\partial B_g(\theta^e_{j+1/2})}{\partial \theta^e_{j+1/2}},$$

$$\frac{\partial \dot{u}_{gj+1/2}}{\partial u_{gj+3/2}} = \frac{A_{j+1}}{V_{j+1/2}} \left[a^r_{gj+1} + (u_{gj+1/2} - u_{gj+3/2}) \frac{\partial a^r_{gj+1}}{\partial u_{gj+3/2}} \right],$$

$$\frac{\partial \dot{\theta}^i_{j+1/2}}{\partial \theta^i_{j-1/2}} = \frac{A_j}{\rho_{j+1/2} c^i_{vj+1/2} V_{j+1/2}} \left[a^i_j + (\theta^i_{j-1/2} - \theta^i_{j+1/2}) \frac{\partial a^i_j}{\partial \theta^i_{j-1/2}} \right],$$

$$\frac{\partial \dot{\theta}^i_{j+1/2}}{\partial \theta^i_{j+1/2}} = - \frac{A_j}{\rho_{j+1/2} c^i_{vj+1/2} V_{j+1/2}} \left\{ A_j \left[a^i_j - (\theta^i_{j-1/2} - \theta^i_{j+1/2}) \frac{\partial a^i_j}{\partial \theta^i_{j+1/2}} \right] \right.$$

$$\left. + A_{j+1} \left[a^i_{j+1} - (\theta^i_{j+1/2} - \theta^i_{j+3/2}) \frac{\partial a^i_{j+1}}{\partial \theta^i_{j+1/2}} \right] \right\} - \omega^{ie}_{j+1/2},$$

$$\frac{\partial \dot{\theta}^i_{j+1/2}}{\partial \theta^e_{j+1/2}} = w^{ie}_{j+1/2},$$

$$\frac{\partial \dot{\theta}^i_{j+1/2}}{\partial \theta^e_{j+3/2}} = \frac{A_{j+1}}{\rho_{j+1/2} c^i_{vj+1/2} V_{j+1/2}} \left[a^i_{j+1} + (\theta^i_{j+1/2} - \theta^i_{j+3/2}) \frac{\partial a^i_{j+1}}{\partial \theta^i_{j+3/2}} \right],$$

$$\frac{\partial \dot{\theta}^e_{j+1/2}}{\partial \theta^e_{j-1/2}} = \frac{A_j}{\rho_{j+1/2} c^e_{vj+1/2} V_{j+1/2}} \left[a^e_j + (\theta^e_{j-1/2} - \theta^e_{j+1/2}) \frac{\partial a^c_j}{\partial \theta^e_{j-1/2}} \right],$$

$$\frac{\partial \dot{\theta}^e_{j+1/2}}{\partial u_{gj+1/2}} = \frac{c}{\rho_{j+1/2} c^e_{vj+1/2}} \left\{ \sigma^a_{gj+1/2}(\theta^e_{j+1/2}) \right.$$

$$+ \frac{v_g - v_{g-1}}{v_g} [\sigma^-_{gj+1/2}(\theta^e_{j+1/2})(\beta_{g-1} u_{g-1,j+1/2} + 1)$$

$$+ \beta_g \sigma^-_{g+1,j+1/2}(\theta^e_{j+1/2}) u_{g+1,j+1/2}]$$

$$- \frac{v_{g+1} - v_g}{v_g} [\sigma^+_{gj+1/2}(\theta^e_{j+1/2})(\beta_{g+1} u_{g+1,j+1/2} + 1)$$

$$\left. + \beta_g \sigma^+_{g-1,j+1/2}(\theta^e_{j+1/2}) u_{g-1,j+1/2}] \right\},$$

$$\frac{\partial \dot{\theta}^{e}_{j+1/2}}{\partial \theta^{i}_{j+1/2}} = \omega^{ie}_{j+1/2} \frac{c^{n}_{vj+1/2}}{c^{e}_{vj+1/2}},$$

$$\frac{\partial \dot{\theta}^{e}_{j+1/2}}{\partial \theta^{e}_{j+1/2}} = -\frac{1}{\rho_{j+1/2} c^{e}_{vj+1/2}} \sum_{g=1}^{G} c\sigma^{a}_{gj+1/2}(\theta^{e}_{j+1/2}) \frac{\partial B_{g}(\theta^{e}_{j+1/2})}{\partial \theta^{e}_{j+1/2}} - \omega^{ie}_{j+1/2} \frac{c^{n}_{vj+1/2}}{c^{e}_{vj+1/2}}$$

$$- \frac{1}{\rho_{j+1/2} c^{e}_{vj+1/2} V_{j+1/2}} \Big\{ A_{j} \left[a^{e}_{j} - (\theta^{e}_{j\ 1/2} - \theta^{e}_{j+1/2}) \frac{\partial a^{e}_{j}}{\partial \theta^{e}_{j+1/2}} \right]$$

$$+ A_{j+1} \left[a^{e}_{j+1} - (\theta^{e}_{j+1/2} - \theta^{e}_{j+3/2}) \frac{\partial a^{e}_{j+1}}{\partial \theta^{e}_{j+1/2}} \right] \Big\},$$

$$\frac{\partial \dot{\theta}^{e}_{j+1/2}}{\partial \theta^{e}_{j+3/2}} = \frac{A_{j+1}}{\rho_{j+1/2} c^{e}_{vj+1/2} V_{j+1/2}} \left[a^{e}_{j+1} + (\theta^{e}_{j+1/2} - \theta^{e}_{j+3/2}) \frac{\partial a^{e}_{j+1}}{\partial \theta^{e}_{j+3/2}} \right].$$

The sparsity pattern of the Jacobian is shown in Fig. 1. We note some approximations made in calculating the Jacobian,

(1) The opacity σ^{a} and the transfer matrix elements $\sigma^{\pm}$ are evaluated at a predicted value of the electron temperature θ^{e} which may differ from that at which the Jacobian is being evaluated.

(2) A number of derivatives are assumed to be zero,

$$\frac{\partial \sigma^{a}}{\partial \theta^{e}} = \frac{\partial \sigma^{\pm}}{\partial \theta^{e}} = \frac{\partial \omega^{ie}}{\partial \theta^{e}} = \frac{\partial a^{r}}{\partial u_{g}} = \frac{\partial a^{e}}{\partial \theta^{e}} = \frac{\partial a^{i}}{\partial \theta^{i}} = 0.$$

(3) Terms proportional to β_{g}, which arise from stimulated Compton scattering, are ignored.

B. *Solution of the Linear Problem*

We wish to solve equations of the form $Cz = l$, where C is a large sparse matrix. C has the same sparsity pattern as the Jacobian matrix for our differential equations. This pattern is illustrated in Fig. 1, where for convenience we have shown only three

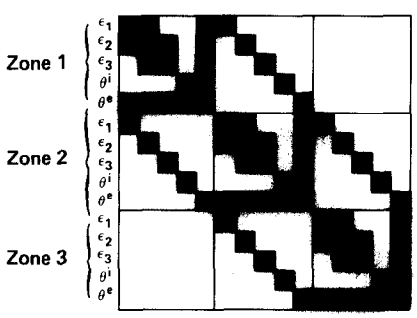

FIG. 1. Sparsity pattern of the Jacobian.

photon energy groups and three zones. The shaded squares denote (possibly) nonzero components.

In general, C is a block tridiagonal matrix. Each diagonal block is a $(G+2)$ by $(G+2)$ matrix, where G is the number of photon energy groups. These diagonal blocks are, in turn, so called *bordered* tridiagonal matrices. That is, they are tridiagonal with additional entries in the last row and column, which correspond to photon–electron interactions in each zone.

The general method of solution is a new one we call "double-splitting iteration." The splitting iteration technique refers to repeated iteration using a matrix M which approximates C in some sense,

$$z_{i+1} = M^{-1}(l - Cz_i) + z_i = M^{-1}[l - (C - M)z_i].$$

This iteration is only feasible if $Mz_{i+1} = l - (C - M)z_i$ is easier to solve than $Cz = l$. If z is the true solution, so that $Cz = l$, then we have

$$Mz_{i+1} = Cz - Cz_i + Mz_i \qquad \text{or} \qquad M(z_{i+1} - z) = (C - M)(z - z_i).$$

Thus if $\|M^{-1}(C - M)\| < 1$, we have $\|z_{i+1} - z\| < \|z - z_i\|$ and the iteration converges. But $M^{-1}(C - M) = M^{-1}C - I$ so that if M is a good approximation to C, $\|M^{-1}C - I\|$ should be small.

A double-splitting iteration is simply a method in which two different M's are used in turn,

$$z_{i+1} = M_2^{-1}[l - (C - M_2)y],$$

where $y = M_1^{-1}[l - (C - M_1)z_i]$. The rate of convergence depends on $\|M_2^{-1}(C - M_2)M_1^{-1}(C - M_1)\|$, which may be smaller than $\|M_2^{-1}(C - M_2)\| * \|M_1^{-1}(C - M_1)\|$. The alternation of the two splittings may be better than repeating either one.

Indeed, we select M_1 and M_2 to represent two distinct aspects of the physics. M_1 and M_2 are shown in Figs. 2 and 3, respectively. M_2 consists of the diagonal blocks of C. M_1 consists of the outer diagonals, the main diagonal of the diagonal blocks, plus the last two rows of the diagonal blocks. Since we first devised this method, a

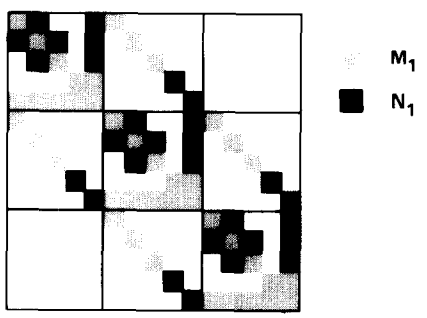

FIG. 2. The first splitting reflects couplings between spatial zones. N_1 labels that part of C not included in M_1.

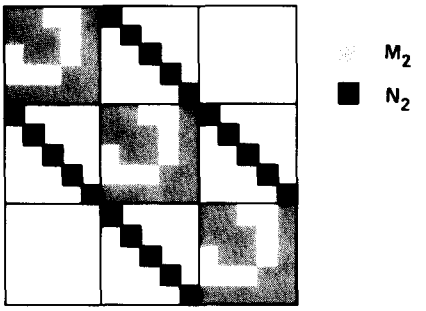

FIG. 3. The second splitting reflects couplings within zones. N_2 labels that part of C not included in M_2.

similar splitting scheme for a somewhat less complicated physical problem has been used by Mihalas, Weaver, and Sanderson [19].

It is easy to solve $M_2 z = y$. It suffices to solve this equation for each diagonal block, and indeed the solutions can be done in parallel on a vector or parallel computer. Since the diagonal blocks are bordered tridiagonal, we can write each block D as a product $D = LU$, where L and U are: L is a lower bidiagonal matrix plus a last row, L has 1's on the diagonal, and U is an upper bidiagonal matrix with an additional last column.

Denoting the tridiagonal part of D by T, and letting R, E, and δ denote the bottom row (less the last element), column (less the last element), and corner element, respectively, L and U can be found as follows:

(1) Write $T = L_1 U_1$; find L_1 and U_1 by the usual L–U decomposition method. By convention, L_1 has unit diagonal.

(2) Solve $L_1 E_1 = E$ for E_1.

(3) Solve $R_1 U_1 = R$ for R_1.

(4) Find $\delta_1 = \delta - R_1 \cdot E_1$.

(5) $L = \begin{pmatrix} L_1 & 0 \\ R_1 & 1 \end{pmatrix}$.

(6) $U = \begin{pmatrix} U_1 & E_1 \\ 0 & \delta_1 \end{pmatrix}$.

The reader may confirm that $LU = \begin{pmatrix} T & E \\ R & \delta \end{pmatrix} = D$ as desired.

The solution of the equation $M_1 z = y$ is a little easier to describe but harder to picture. Note that ignoring the last two rows in each block, the matrix is tridiagonal. Therefore we can solve for all but the last two components (corresponding to the ion and electron temperatures) in each zone. Once these components are known, the last two rows can be reduced to a 2×2 system, which can be solved straightforwardly.

We have gone through the above for completeness, but viewed physically, it is easy to say what is being done. In solving $M_2 z = y$, we are including only the couplings of the matrix which represent processes *within* a zone. Fortunately, the form of those couplings admits an L–U decomposition. In solving $M_1 z = y$, we are solving the

tridiagonal system which represents photon transport *between* zones, then updating the ion and electron temperatures. This view helps one judge that M_1 and M_2 are likely to be excellent approximations of C, especially taken alternately. In fact, in practice convergence has been excellent, typically taking $3-5$ iterations.

If the linear solver has not converged after a reasonable number of steps, it can signal failure to the nonlinear solver and in turn the ordinary differential equation solver will decrease the time step. Thus, failure of this iteration is not fatal at all. Eventually, for a small enough time step M_1 and M_2 will both become excellent approximations to C.

III. Numerical Example

As noted in the Introduction, our primary concern is with errors which arise from the choice of algorithms used to solve the multigroup diffusion form of the radiative transfer equation rather than those which follow from the diffusion approximation itself. Such errors occur from applying operator-splitting techniques without restricting the time step sufficiently to ensure an adequate treatment of the nonlinear processes which are important in obtaining an accurate solution.

For solutions based on a single radiation temperature model, time step controls can be devised to provide almost any desired degree of accuracy. The same cannot be said for the multigroup model with operator splitting. Often one is forced to run with various limits to see if the solution has converged. By contrast, our algorithm does not have this problem.

To illustrate, we have invented a test problem which has vigorous energy production. Consider a 0.002-cm radius sphere filled with deuterium at density 10,000 g/cm^3 and initial temperature 5 keV. The total mass of deuterium is approximately 330 μg. Using the thermonuclear reaction cross section of Chase, LeBlanc, and Wilson [20] we have calculated the thermonuclear burn with both a multigroup operator-splitting code and a multigroup code using our model.

Both codes are one dimensional and Lagrangian with spherical symmetry. In addition to the equations for radiation transport, electron and ion thermal conduction, and radiation-matter coupling, the equations of hydrodynamics with artificial viscosity are solved. All thermonuclear energy is deposited locally and no attempt is made to follow the neutron or helium 3 products of the deuterium reaction. A simple gamma law with a gamma of 5/3 is used as the equation of state for deuterium. Zoning, boundary, and initial conditions are as follows. The deuterium ball is divided into ten equal radial thickness zones from 0–0.002 cm radii. The outer boundary is initially at rest but otherwise free to move. The deuterium is initially uniform in density and at rest.

The state of the problem is advanced in time by finite steps, the length of which are determined by the stability condition for the finite difference equations unless artificially constrained by an input parameter or a maximum growth rate of 20%. Typical unconstrained time steps are $1-5\times10^{-13}$ sec and for a problem duration of

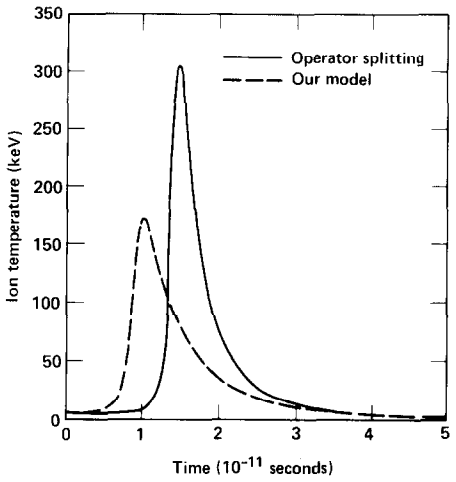

FIG. 4. Ion temperature at the center of a deuterium ball in keV versus elapsed time in seconds for operator splitting and for the model discussed in the text.

5×10^{-11} sec, over 300 time steps are required. The initial time step is 1×10^{-14} sec. A summary of the results of the computer calculations is given in Figs. 4 and 5.

Figure 4 is a plot of the central ion temperature in keV as a function of elapsed time in seconds for both models. The operator-splitting result appears to be both time delayed and overheated. Although not apparent in this particular calculation, operator-splitting results tend to be somewhat noisy. Since the thermonuclear reaction rates and transport coefficients have strong temperature dependence, the time

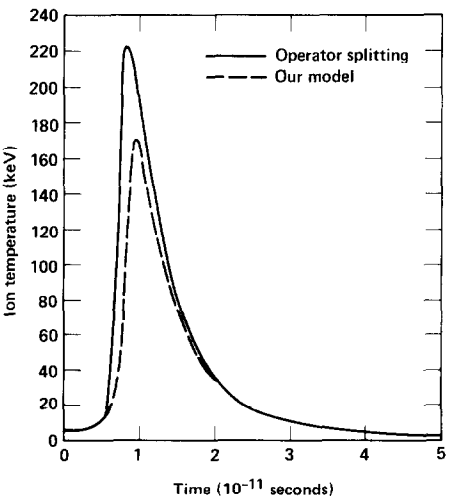

FIG. 5. Ion temperature at the center of a deuterium ball in keV versus elapsed time in seconds for operator splitting restricted to a time step of 5×10^{-14} sec and for the model discussed in the text.

evolutions of the two calculations are quite different. Both calculations took 310 time steps to run to 5×10^{-11} sec. The operator-splitting code used 0.695 min of computer time, while our model code used 0.831 min of computer time.

Figure 5 is a plot similar to that of Fig. 4. In this case, however, the operator-splitting calculation has been restricted to a time step of 5×10^{-14} sec. The time evolutions of both calculations are similar. Operator splitting overpredicts the ion temperature, and gives a smooth but incorrect solution. The operator-splitting code ran 1020 cycles and used 2.46 min of computer time compared with 0.831 min for our model. Further reductions of the time step by a factor of 10 in the operator-splitting calculation yield results which converge to those predicted by our algorithm.

IV. Conclusion

Our model has been used to address a variety of test problems. They include those dominated by photon–matter coupling, Compton scattering, or radiation transport, as well as those in which two or three of these physical processes are significant. This provides a considerable experience base for evaluating the strengths and weaknesses of the algorithm. The major strength of the method is clearly its ability to produce reliably an accurate solution of the physics model each time it is run. This is of particular value given the fact that the relative importance of, and coupling stengths between, the physical processes included in the model vary radically from problem to problem. Operator-splitting schemes do not exhibit the same robustness. It has required considerable effort to achieve this robustness, which is directly attributable to the use of a general ordinary differential equation solver, while retaining acceptable execution speed.

The execution speed of our model is markedly superior to operator-splitting methods on difficult problems when the comparison is made on the basis of equal accuracy. On easy problems the situation is reversed, with our model being somewhat slower. Even this disadvantage is largely eliminated by the fact that it is necessary to rerun the operator-splitting methods with a smaller time step to ensure that the problem is in fact easy and that the solution has converged.

Acknowledgments

The authors wish to express indebtedness to Alan Hindmarsh for valuable discussions.

References

1. M. L. Alme and J. R. Wilson, *Astrophys. J.* **186** (1973), 1015.
2. C. M. Lund and J. R. Wilson, "Some Numerical Methods for Time-Dependent Multifrequency Radiation Transport Calculation in One Dimension," No. UCRL-84678, Lawrence Livermore National Laboratory, Livermore, Calif. 1980.

3. J. I. CASTOR, *Astrophys. J.* **178** (1972), 779.
4. R. W. LINDQUIST, *Ann. Phys.* **37** (1966), 487.
5. J. R. BUCHLER, *J. Quant. Spectrosc. Radiat. Transfer* **22** (1979), 293.
6. C. D. LEVERMORE, "A Capman–Enskog Approach to Flux-Limited Diffusion Theory," No. UCID-18229, Lawrence Livermore National Laboratory, Livermore, Calif., 1979.
7. G. C. POMRANING, "A Comparison of Various Flux Limiters and Eddington Factors," No. UCID-19220, Lawrence Livermore National Laboratory, Livermore, Calif., 1981.
8. G. C. POMRANING, *J. Quant. Spectrosc. Radiat. Transfer* **27** (1982), 517.
9. C. D. LEVERMORE AND G. C. POMRANING, *Astrophys. J.* **248** (1981), 321.
10. G. E. COOPER, "A Fine Structure Generalization of the Compton Fokker Planck Equation," No. UCIR-509, Lawrence Livermore National Laboratory, Livermore, Calif., 1970.
11. G. E. COOPER, *Phys. Rev. D* **3** (1971), 2312.
12. A. S. KOMPANEETS, *Sov. Phys. JETP* **4** (1973), 730.
13. S. STONE, "Compton Scattering at High Material Temperatures," No. UCRL-73424 Lawrence Livermore National Laboratory, Livermore, Calif., 1971.
14. A. M. WINSLOW, "Implicit Numerical Methods for Compton Scattering Energy Exchange Between Electrons and Non-Planckian Radiation," No. UCID-16854, Lawrence Livermore National Laboratory, Livermore, Calif., 1976.
15. J. S. CHANG AND G. E. COOPER, *J. Comput. Phys.* **6** (1970), 1.
16. A. C. HINDMARSH, "Preliminary Documentation of GEARBI: Solution of ODE Systems with Block-Iterative Treatment of the Jacobian," No. UCID-30149, Lawrence Livermore National Laboratory, Livermore, Calif., 1976.
17. C. W. GEAR, "Numerical Initial Value Problems in Ordinary Differential Equations," Prentice–Hall, Englewood Cliffs, N. J., 1971.
18. T. S. AXELROD, P. F. DUBOIS, R. B. HICKMAN, A. C. HINDMARSH, AND J. F. PAINTER, "TORANAGA," No. UCID-30190, Lawrence Livermore National Laboratory, Livermore, Calif., 1983.
19. D. MIHALAS, R. P. WEAVER, AND J. G. SANDERSON, *J. Quant. Spectrosc. Radiat. Transfer* **28** (1982), 53.
20. J. B. CHASE, J. M. LEBLANC, AND J. R. WILSON, *Phys. Fluids* **16** (1973), 1142.